Electronic Supplementary Material (ESI) for Physical Chemistry Chemical Physics.

UV and VUV-induced fragmentation of tin-oxo cage ions

Jarich Haitjema, Lianjia Wu, Alexandre Giuliani, Laurent Nahon, Sonia Castellanos, and Albert M. Brouwer

Electronic Supplementary Information

Content

Additional data

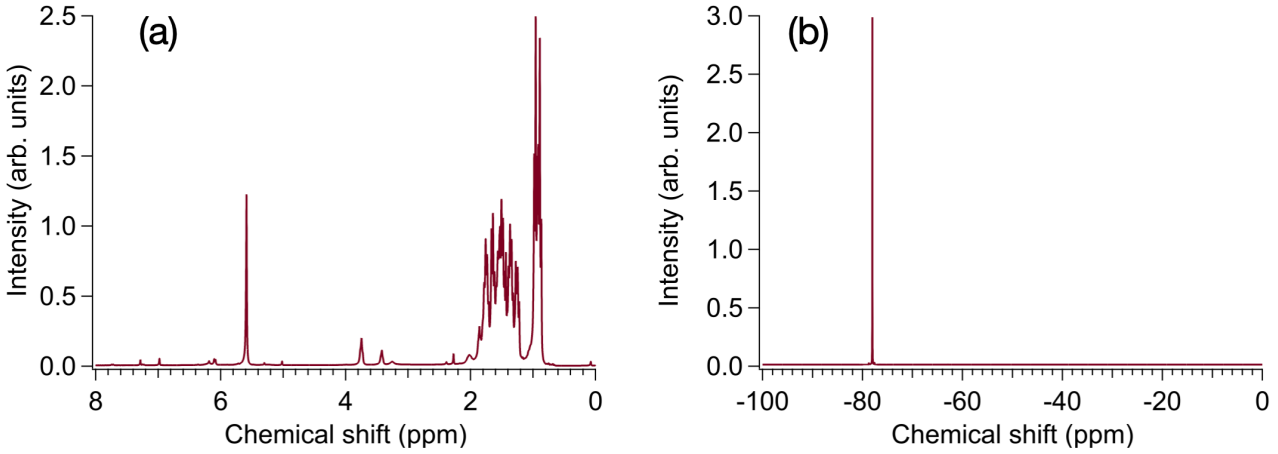

Fig. S1 (a) ^{1}H NMR spectrum and (b) ^{19}F NMR spectrum of TinOTf in CD_2Cl_2. The ^{1}H NMR shows the signals corresponding to butyl groups of the tin-oxo cage,[1] and a signal for CD_2Cl_2 (5.4 ppm). The ^{19}F spectrum shows that only one type of fluorine atoms is present in the material.

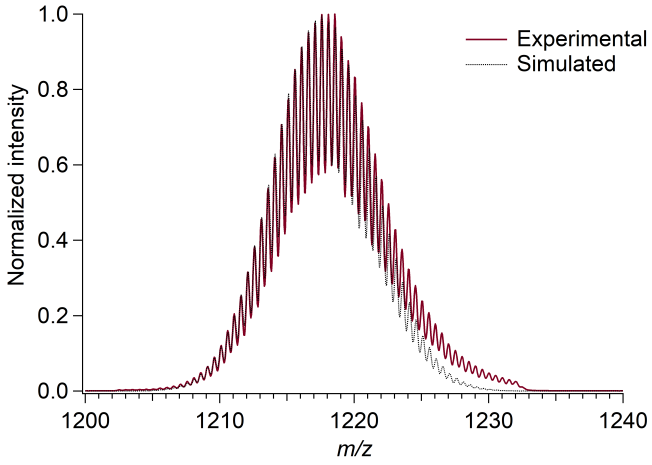

Fig. S2 Electrospray ionization (ESI) mass spectrum of $[(n\text{BuSn})_{12}O_{14}(OH)_6]^{2+}$ (M^{2+}), showing the precursor peak centered at m/z 1218. This experimental spectrum is an average of the 36 photofragmentation spectra in the range 4.1–7.6 eV. The precursor peak did not show a significant difference at different incident photon energies. For comparison, the dotted line shows a spectrum predicted by the online tool "Chemcalc" (resolution: 3200, full width half max. ≈ 0.38).[2]

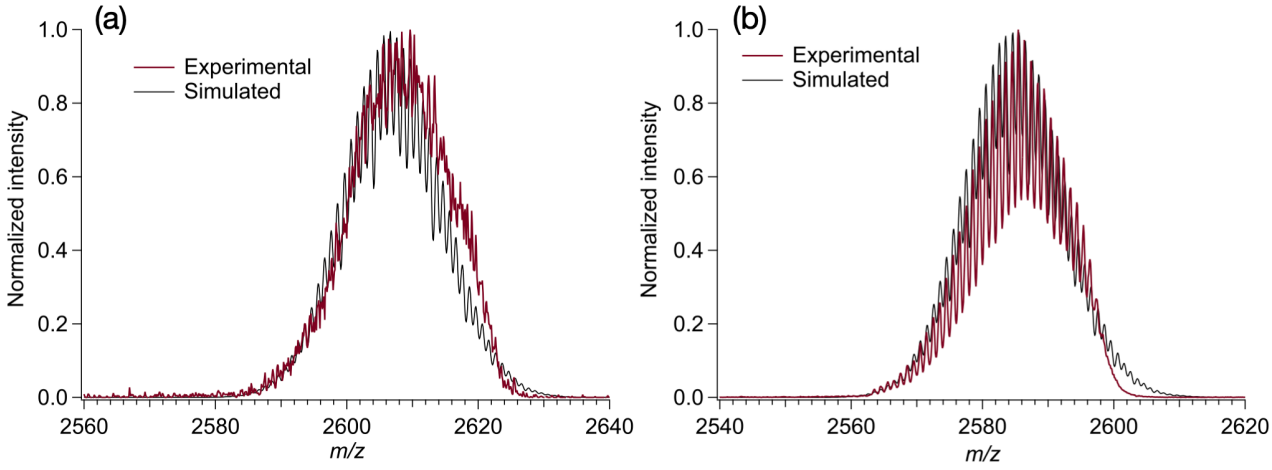

Fig. S3 Mass spectra of the precursor peaks (a) $MOTf^+$ and (b) $MOTs^+$. The black lines show simulated spectra using the online tool "Chemcalc" (resolution: 3200, full width half max. ≈ 0.81).[2]

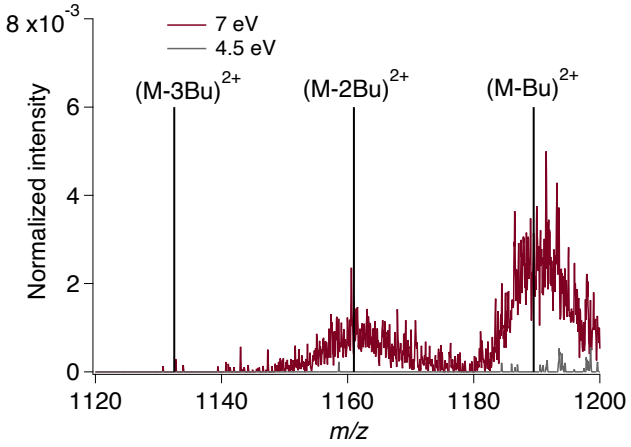

Fig. S4 Photofragmentation spectrum of the tin-oxo cage dication at 7 eV (red) and 4.5 eV (gray). It can be seen that the 4.5 eV spectrum does not show a clear $(M–Bu)^{2+}$ or $(M–2Bu)^{2+}$ peak: the non-zero area between m/z 1175 and 1203 is due to spectral noise.

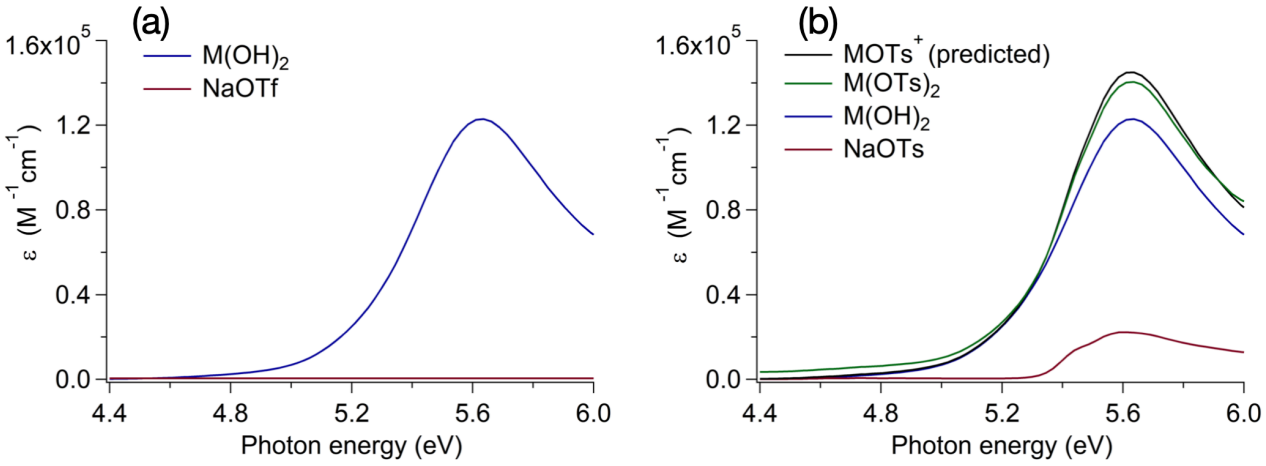

Fig. S5 UV/Vis absorption spectra of the counterions (a) triflate and (b) tosylate, measured in their sodium salt form in H_2O (for NaOTf) and in EtOH (for NaOTs). For tosylate, a prediction for the absorption spectrum of the monocation $TinOTs^+$ is also given, calculated by adding the NaOTs and TinOH ($M(OH)_2$) spectra together. The experimental spectrum of TinOTs, $M(OTs)_2$, is shown as well.

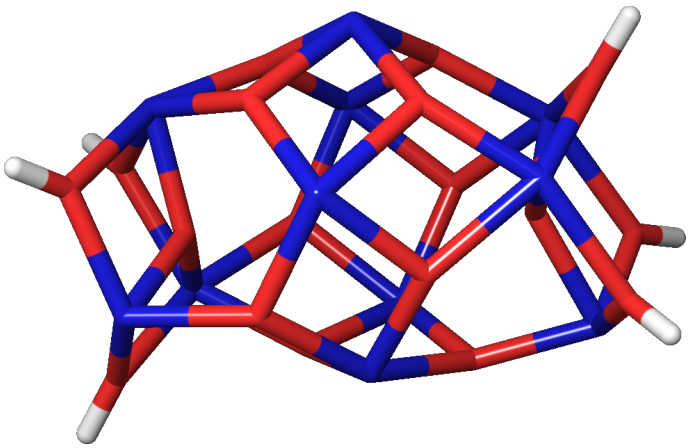

Fig. S6 Possible structure of the species $(M\text{-}Bu\text{-}SnO_2)^{3+}$ (m/z 743). Butyl groups not shown for clarity.

Detailed results of quantum chemical calculations

Geometries were optimized at the B3LYP/LANL2DZ level. Zero-point vibrational energies were obtained at the same level. Single point Def2SVP and De2TZVP calculations were used for better evaluation of relative energies. All calculations were initiated from one low-energy conformer of the *n*-butyl tin cage (M^{2+}). It cannot be excluded that lower-energy conformers (formed by rotation about the Sn-C bonds) can be found for any of the structures computed in this work. The energy differences involved are typically < 0.05 eV, so they are unlikely to be relevant for the main conclusions.

To obtain M-Bu one of the butyl groups of the six-coordinated tin atoms was removed. Energies and structures of the isomers in which a butyl was removed from a five-coordinated tin atom are also supplied.

The second butyl group was taken from the same side of the molecule. For the 2+ species this leads to a closed-shell species after rearrangement of a bridging OH group. Other regioisomers gave higher energies, and are not reported here. For the 3+ series, the M-2Bu species are distonic radical ions, and the difference in energies between different isomers is smaller.

Further dealkylation was first explored using the methyltin oxo cage as a simplified model system. In this work we only report the M-3Bu species, in which all butyl groups come from the same side of the molecule.

Table S1 contains the description of the species, with their charge and spin state, and the energies. The structures are provided as individual plain text files in mol2 format which can be read by many molecular visualization programs. Images of all tin cage structures are provided in Figure S7.

Table S1. Detailed results of DFT calculations.[3] For each species, characterized by structure, charge, and spin, the name is given of the mol2 structure file, the energy (a.u.) at the B3LYP// LANL2DZ level, the zero point vibrational energy, and the single point Def2SVP and Def2TZVP energies.

species	charge	spin	file name	E(LANL2DZ)	ZPE	E(Def2SVP)	E(Def2TZVP)
M	2	1	M_2_1	-3443.74429	1.62208	-5972.62170	-5976.69876
M	3	2	M_3_2	-3443.31161	1.61979	-5972.19594	-5976.27617
M-Bu	2	2	M-Bu_2_2	-3285.87572	1.49853	-5814.85595	-5818.75898
M-Bu (5-coord)	2	2	M-Bu_2_2_5Sn	-3285.87081	1.49874	-5814.85143	-5818.75345
M-Bu	3	1	M-Bu_3_1	-3285.50558	1.49925	-5814.48792	-5818.39661
M-Bu (5-coord)	3	1	M-Bu_3_1_5Sn	-3285.46203	1.49915	-5814.45710	-5818.36313
M-2Bu	2	1	M-2Bu_2_1	-3128.04056	1.37428	-5657.12971	-5660.86836
M-2Bu	3	2	M-2Bu_3_2	-3127.63446	1.37581	-5656.71901	-5660.45387
M-3Bu	2	2	M-3Bu_2_2	-2970.17329	1.25034	-5499.36583	-5502.93045
M-3Bu	3	1	M-3Bu_3_1	-2969.81757	1.25079	-5498.99524	-5502.56830
MOMs	1	1	MOMs_1_1	-3719.51353	1.67223	-6636.25935	-6640.82994
MOMs	2	2	MOMs_2_2	-3719.18060	1.67028	-6635.92988	-6640.50038
MOMs-Bu-1[a]	1	2	MOMs-Bu_1_2-a	-3561.64647	1.54858	-6478.49317	-6482.89173
MOMs-Bu-2[b]	1	2	MOMs-Bu_1_2-b	-3561.64607	1.54867	-6478.49498	-6482.89199
MOMs-Bu	2	1	MOMs-Bu_2_1	-3561.43778	1.55029	-6478.26236	-6482.66462
MOMs-2Bu[a]	1	1	MOMs-2Bu_1_1-a	-3403.82658	1.42313	-6320.77466	-6325.01000
MOMs-2Bu[b]	1	1	MOMs-2Bu_1_1-b	-3403.81445	1.42446	-6320.77279	-6325.00453
MOMs-2Bu	2	2	MOMs-2Bu_2_2	-3403.56825	1.42681	-6320.49528	-6324.72371
MOTf	1	1	MOTf_1_1	-4017.20467	1.64699	-6933.72485	-6938.66247
MOTf	2	2	MOTf_2_2	-4016.86437	1.64547	-6933.38953	-6938.32700
MOTf-Bu-1[a]	1	2	MOTf-Bu_1_2-a	-3859.33711	1.52325	-6775.95785	-6780.72367
MOTf-Bu-1[b]	1	2	MOTf-Bu_1_2-b	-3859.33764	1.52357	-6775.95937	-6780.72431
MOTf-Bu	2	1	MOTf-Bu_2_1	-3859.11633	1.52466	-6775.71784	-6780.48701
MOTf-2Bu[a]	1	1	MOTf-2Bu_1_1-a	-3701.51953	1.39776	-6618.24247	-6622.84120
MOTf-2Bu[b]	1	1	MOTf-2Bu_1_1-b	-3701.50491	1.39917	-6618.23771	-6622.83641
Bu	0	2	butyl	-157.76222	0.11747	-157.67084	-157.84783
M-Bu-SnO2	3	1	M-Bu-SnO2	-3131.47197			

[a] Bu removed from the side to which anion is bound [b] Bu removed from side opposite to the one to which the anion is bound.

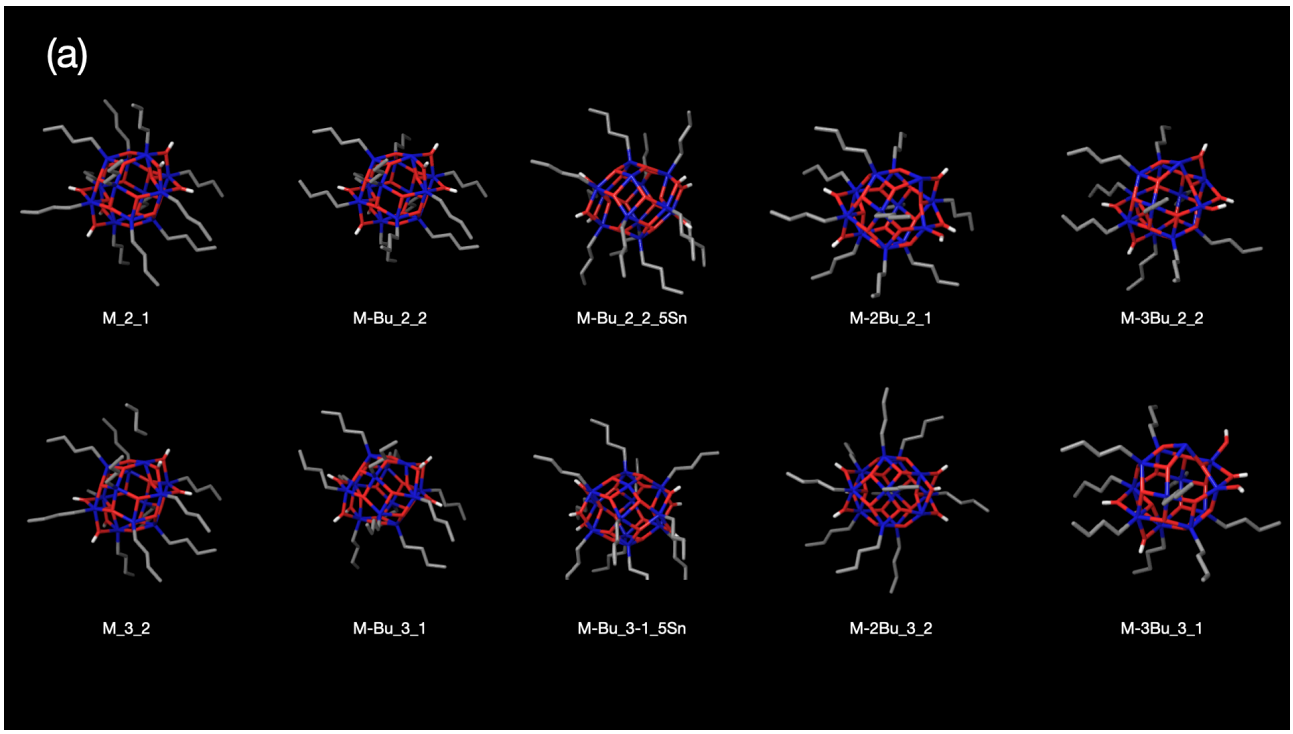
(a)
M_2_1
M-Bu_2_2
M-Bu_2_2_5Sn
M-2Bu_2_1
M-3Bu_2_2
M_3_2
M-Bu_3_1
M-Bu_3-1_5Sn
M-2Bu_3_2
M-3Bu_3_1

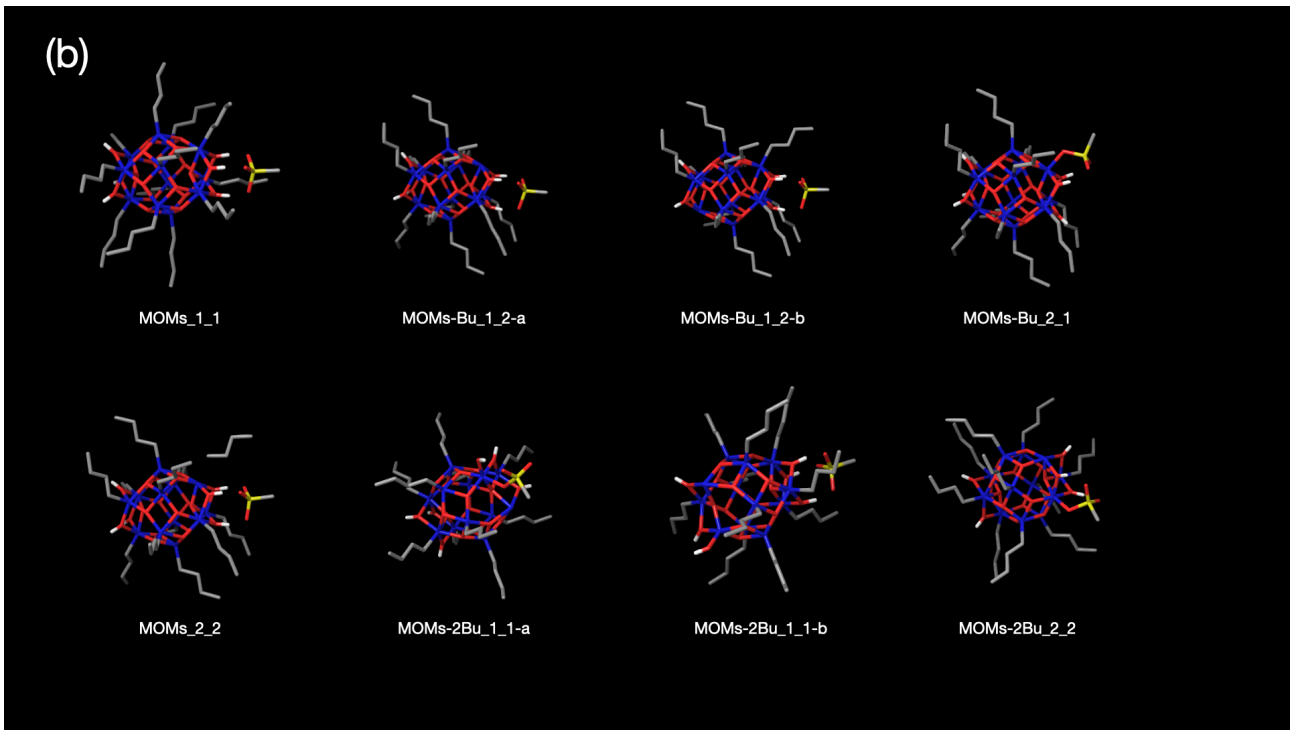
(b)
MOMs_1_1
MOMs-Bu_1_2-a
MOMs-Bu_1_2-b
MOMs-Bu_2_1
MOMs_2_2
MOMs-2Bu_1_1-a
MOMs-2Bu_1_1-b
MOMs-2Bu_2_2

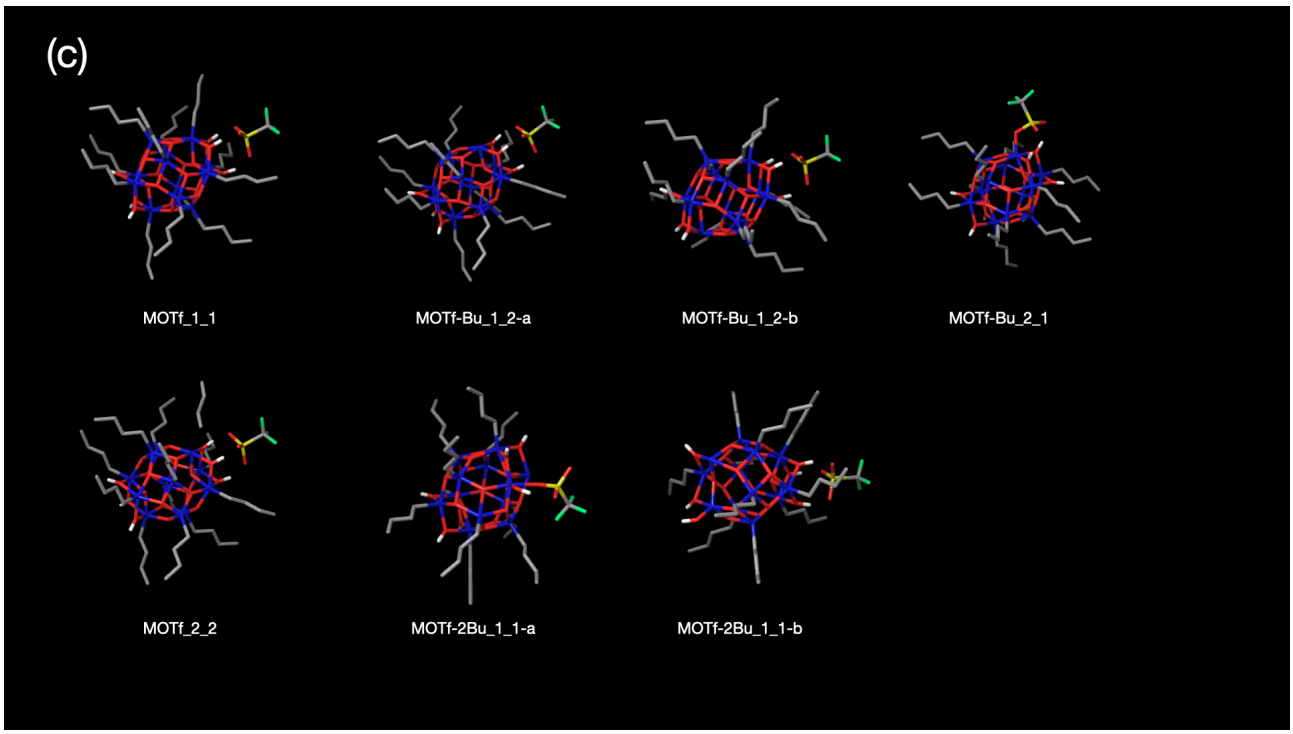

Fig. S7 Images of the computed structures. (a) tin cages without counter ion (b) OMs counter ion, (c) OTf counter ion

References

1. F. Banse, P. Toledano, J. Maquet and C. Sanchez, Inorg. Chem., 1995, 34, 6371–6379.
2. L. Patiny and A. Borel, J. Chem. Inf. Model., 2013, 53, 1223–1228.
3. M. J. Frisch, G. W. Trucks, H. B. Schlegel, G. E. Scuseria, M. A.Robb, J. R. Cheeseman, G. Scalmani, V. Barone, G. A. Peters-son, H. Nakatsuji, X. Li, M. Caricato, A. V. Marenich, J. Bloino,B. G. Janesko, R. Gomperts, B. Mennucci, H. P. Hratchian,J. V. Ortiz, A. F. Izmaylov, J. L. Sonnenberg, D. Williams-Young, F. Ding, F. Lipparini, F. Egidi, J. Goings, B. Peng,A. Petrone, T. Henderson, D. Ranasinghe, V. G. Zakrzewski,J. Gao, N. Rega, G. Zheng, W. Liang, M. Hada, M. Ehara,K. Toyota, R. Fukuda, J. Hasegawa, M. Ishida, T. Nakajima, Y. Honda, O. Kitao, H. Nakai, T. Vreven, K. Throssell, J. A.Montgomery, Jr., J. E. Peralta, F. Ogliaro, M. J. Bearpark, J. J.Heyd, E. N. Brothers, K. N. Kudin, V. N. Staroverov, T. A.Keith, R. Kobayashi, J. Normand, K. Raghavachari, A. P. Ren-dell, J. C. Burant, S. S. Iyengar, J. Tomasi, M. Cossi, J. M.Millam, M. Klene, C. Adamo, R. Cammi, J. W. Ochterski, R. L.Martin, K. Morokuma, O. Farkas, J. B. Foresman and D. J. Fox, Gaussian 16 Revision A.03, 2016.